Journal of Dentistry and Oral Biology

Research Article
Published: 25 Apr, 2020

Mechanical Interlocking Capacity of Titanium with Respect to Surface Morphology and Topographical Parameters

Mitsunori Uno[1], Marc Hayashi[2], Ryotaro Ozawa[1], Juri Saruta[1], Hajime Ishigami[3] and Takahiro Ogawa[1]*

[1]Division of Advanced Prosthodontics, Weintraub Center for Reconstructive Biotechnology, UCLA School of Dentistry, Los Angeles, USA

[2]Section of Restorative Dentistry, Division of Constitutive and Regenerative Sciences, UCLA School of Dentistry, Los Angeles, USA

[3]Department of Prosthodontics, Division of Oral Functional Science and Rehabilitation, Asahi University School of Dentistry, Gifu, Japan

Abstract

Purpose: Osseointegration, which can be considered as the direct contact between living bone and implant surfaces, is critical to implant anchorage. This study was aimed at evaluating the mechanical interlocking at titanium interfaces (*via.* shear tests) with respect to the surface morphology, and for determining the primary contributing factors.

Methods: Shear tests were performed on five different titanium surfaces, namely: 1) machined, 2) sandblasted with Al_2O_3, 3) acid-etched, 4) sandblasted with Al_2O_3 and acid-etched, and 5) sandblasted with TiO_2 and acid-etched. Further, commercially available bone cement was used as the mock bone.

Results: Amongst the five tested surfaces, a four-fold difference in the interfacial shear strength was observed, with the machined surface and the sandblasted acid-etched surface exhibiting the lowest and the highest values, respectively. Multiple regression analysis indicated that the developed interfacial area ratio (*Sdr*) was the primary determining factor, which contributed to 60% of the interfacial shear strength; whereas, the average roughness (*Sa*), which is the most commonly used parameter in the field, contributed to only 12% of the interfacial shear strength.

Conclusion: The results revealed that there were significant differences between the mechanical interlocking capacities of the titanium samples with various surface morphologies; this indicated that the anchorage of dental implants with the same bone-to-implant contact can differ significantly. The developed interfacial area ratio (*Sdr*) was therefore proposed as a reliable parameter for the determination of the interlocking capacity of titanium with bone.

Keywords: Titanium; Surface morphology; Spectroscopy; Mechanical interlocking

OPEN ACCESS

Correspondence:
Marc Hayashi, Section of Restorative Dentistry, Division of Constitutive and Regenerative Sciences, UCLA School of Dentistry, 10833 Le Conte Avenue (CHS), Box: 951668, Los Angeles, CA, USA, Tel: (310) 825- 4855; E-mail: mhayashi@dentistry.ucla.edu

Received Date: *03 Apr 2020*
Accepted Date: *22 Apr 2020*
Published Date: *25 Apr 2020*

Citation:
Uno M, Hayashi M, Ozawa R, Saruta J, Ishigami H, Ogawa T. Mechanical Interlocking Capacity of Titanium with Respect to Surface Morphology and Topographical Parameters. J Dent Oral Biol. 2020; 5(2): 1163.
ISSN: 2475-5680

Copyright *© 2020 Marc Hayashi. This is an open access article distributed under the Creative Commons Attribution License, which permits unrestricted use, distribution, and reproduction in any medium, provided the original work is properly cited.*

Introduction

Osseointegration is described as the direct contact between living bone and an implant surface [1]. This contact and interface is a critical factor in implant anchorage [2], which contributes to the overall effectiveness of the prosthesis. Although additional factors influence the implant anchorage and stability such as the bone density and quality as well as skill level of the operator, the implant is critical to the realization of osseointegration [3]. The major implant parameters include the shape, design, and surface characteristics [3-6]. In particular; the surface characteristics of dental implants facilitate the realization of bone apposition at the microscopic scale with respect to the degree of roughness [7]. The most commonly used feature/parameter for the assessment of osseointegration is the Bone to Implant Contact (BIC). The BIC is a histological parameter determined by calculating the percentage of bone coverage that juxtaposes the implant surface without being interposed by soft tissue [8]. In an ideal case, the BIC should be sufficiently high to allow for a load bearing prosthesis to be placed and maintained, as it contributes to the long-term effectiveness of the implant [4,9]. However, it is unclear as to whether the same BIC value results in the same anchoring capacity of implants. As reported by Ito et al. [10], the BIC does not correspond with

Table 1: Surface roughness parameters analyzed in this study. This table presents the classification, symbols, denotations, and definitions of the surface roughness parameters.

Classification	Symbol	Name	Definition
Amplitude/ height parameters	***Sa***	Average roughness/ Arithmetic mean height	The arithmetical mean of the absolute value of height.
	Sz	Maximum height/ Peak-to-valley roughness	The sum of the maximum peak height value and the maximum pit depth value.
	Sku	Kurtosis	A measure of the sharpness of the roughness profile. The higher the value, the sharper the height profile.
	Ssk	Skewness	The degree of profile skews and expresses the symmetry of peaks and valleys using the average line as the center. Rsk=0: Symmetrical about the average line. Rsk >0: skewed downward relative to the average line.
Spatial parameters	***Str***	Texture aspect ratio	A measure of uniformity of the surface texture, a range from 0 to 1. Str >0.5 indicates strong isotropy, while Str <0.3 indicates strong anisotropy
Hybrid parameters	***Sdr***	Developed interfacial area ratio	The percentage of the definition area's additional surface area contributed by the texture as compared to the projected, planar definition area.
	Sdq	Root mean square gradient	A root mean square of slopes at all points in the definition area.

Surface texture parameters in ISO25178

the results obtained by Resonance Frequency Analysis (RFA) with respect to implant anchorage, and a discrepancy between the two commonly utilized parameters was observed. Degidi et al. [11] further reported a non-correlation between the RFA values and BIC. Moreover, a similar finding was reported by Al-Nawas et al. [12] thus, the BIC can be considered as non-reliable for the determination of the load-bearing capacity of implants, which necessitates that another factor is required for elucidating the load-bearing capacity. Although surface roughness contributes significantly to the strength of osseointegration [13], the extent of its influence is unclear with respect to the anchoring capacity of implants. In general, with an increase in the surface roughness, the degree of osseointegration increases. Hence, it is necessary to determine the relationship between the surface roughness's and implant stability. The average roughness (*Sa*) is a parameter commonly used for the representation of the surface roughness of dental implants. Moreover, *Sa* is the arithmetic average of the absolute values of the roughness profile ordinates. However, the assessment of surface morphology using multiple parameters is required in the field of material science, and *Sa* only expresses the vertical profile of the surfaces. An alternative measurement method involves of the developed interfacial ratio (*Sdr*), which is a hybrid parameter that provides information on the number and heights of peaks on an implant surface with respect to the horizontal and space-related characteristics of the surface roughness [14].

The aim of this study was to determine whether the same interfacial shear strength is generated by the same bone coverage, and to elucidate the primary factor that facilitates the effectiveness of osseointegration based on parameters such as the *Sdr, Sa*, and *Sz*. Five different roughness conditions were applied to titanium surfaces, and the bone material (bone cement) was simulated as per the general standards adopted in orthopedic surgeries [15]; this was aimed at the realization of an identical bone coverage. Subsequently, the bone cement was sheared to assess the interfacial strength.

Materials and Methods

Titanium sample preparation

In this study, 30 commercially pure Grade 2 titanium disks (diameter: 20 mm, thickness: 1.5 mm) were separated into five groups (n=6). The machined (*Ma*) surface group served as the control group. Disks *SB (Al)* were subjected to alumina sandblasting (particle diameter: 50 μm) for 3 min at an injection pressure of 0.3 MPa on the *Ma* surface. Disks *AE* were acid-etched using 67% (w/w) H_2SO_4 (Sigma-Aldrich, St. Louis, MO) for 75 s at 110°C on the *Ma* surface. Disks *SB (Al) AE* were subjected to alumina sandblasting (particle diameter: 50 μm) for 3 min at an injection pressure of 0.3 MPa on the *Ma* surface, and then acid-etched using 67% (w/w) H_2SO_4 (Sigma-Aldrich, St. Louis, MO, USA) for 75 s at 110°C. Disks *SB (Ti) AE* were subjected to titanium sandblasting (particle diameter: 149 μm) for 3 min at an injection pressure of 0.3 MPa, and then acid-etched using 67% (w/w) H_2SO_4 (Sigma-Aldrich, St. Louis, MO) for 75 s at 110°C on the *Ma* surface. Thereafter, all the disks were placed in a sealed container and stored for four weeks in a dark room (23°C, 60% humidity).

Titanium surface characterization

The surface morphologies of the *Ma*, *SB (Al)* , *AE*, *SB (Al) AE*, and *SB (Ti) AE* surfaces were examined using Scanning Electron Microscopy (SEM) (Nova 230 Nano SEM, FEI, Hillsboro, OR, USA). The surface roughness was determined with respect to seven different parameters, as follows: the average roughness (*Sa*), maximum height (*Sz*), developed interfacial area ratio (*Sdr*), root mean square gradient (*Sdq*), texture aspect ratio (*Str*), kurtosis (*Sku*),and skewness *(Ssk)* (Table 1). All the samples were measured using an optical surface profiler (Nanto Co., Ltd.).

Shear test of the titanium-bone cement interface

To simulate osseous conditions, Endurance bone cement (DePuy CMW, United Kingdom) was utilized. The bone cement primarily consisted of Polymethyl Methacrylate (PMMA) powder and Methyl Methacrylate (MMA) liquid. Moreover, it was mixed for 20 s (320 μl of liquid and 0.5326 g of powder) and placed into a mold for the fabrication of cylindrical columns (diameter: 2 mm, height: 3 mm). The adhesion interface was then polished using SiC sandpaper (#600). The columns were set apart at 37°C for seven days, thus allowing for polymerization to occur. Thereafter, the pre-fabricated columns were attached to the titanium disks using a fresh mixture of the bone cement, and then further polymerized for 24 h at a load of 1 kg.

A testing machine (Instron 5544, Canton, MA) equipped with a load cell of 1,000 N was used to individually detach the bone cement column from the titanium disks at a crosshead speed of 1 mm/min. The shear stress (units: N) is shown in Figure 1.

Morphology of the bone cement-titanium interface after shear testing

To examine the titanium–bone cement detachment behavior, the titanium surfaces were examined after the shear testing using SEM (JSM-5900LV, Joel Ltd., Tokyo, Japan) and Energy Dispersive X-ray Spectroscopy (EDS) (Nova 230 Nano SEM, Hillsboro, OR, USA).

Statistical analysis

A one-way analysis of variance (ANOVA) was used to assess the

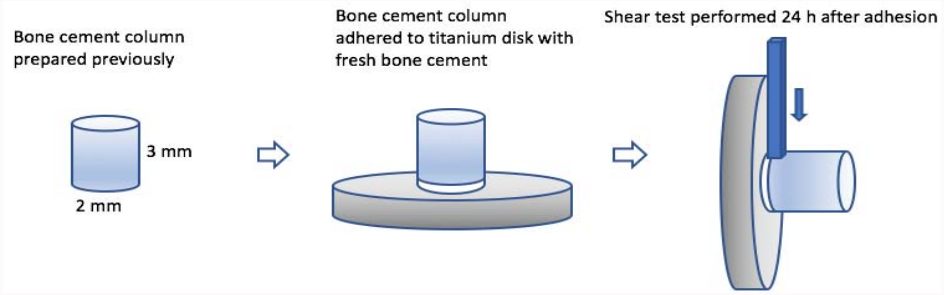

Figure 1: Schematic process of shear test preparation. A testing machine (Instron 5544, Canton, MA) equipped with a load cell of 1,000 N was used to individually detach the bone cement column from the titanium disks at a crosshead speed of 1 mm/min.

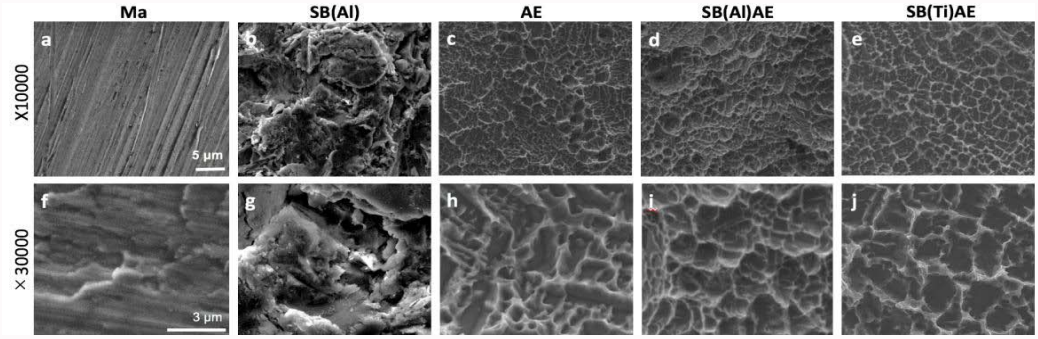

Figure 2: Surface morphologies of titanium surfaces used in this study. Scanning electron micrographs of the *Ma* (a, f), *SB* (Al) (b, g), *AE* (c, h), *SB (Al) AE* (d, i) and *SB (Ti) AE* (e, j). Bar=5 µm in (a,b,c,d, and e), and 3 µm in (f,g,h,i, and j).

influence of the titanium surface roughness and the cement-titanium interfacial shear strength. A Bonferroni multiple comparison was then conducted as the post-hoc test. All the data were expressed as the groups mean ± standard deviation. Moreover, the results with probability levels of 0.05 or less were considered significant. A correlation analysis between the surface roughness and interfacial shear strength values was then conducted, in addition to multiple regression analysis, using SPSS software (IBM Corp., Armonk, NY, USA).

Results

Titanium surface morphology

The SEM images (Nova 230 Nano SEM, Hillsboro, OR, USA) of the titanium surfaces after treatment are shown in Figure 2. At a magnification of 10000x, concentric ridges on the machined surface can be observed (Figure 2A), whereas a uniformly rough surface can be observed on the remaining treated surfaces (Figures 2B-2E). At a magnification of 30000x, the microscopic roughness can be better observed, with significant peaks and valleys on the *AE*, *SB (Al) AE*, and *SB (Ti) AE* surfaces (Figures 2H-2J).

Quantitative topographical evaluations of titanium surfaces

To identify significant differences between the surface morphologies of the five surfaces, quantitative assessments of the 3-dimensional profiles were conducted. Of all the surface treatments, *SB (Al) AE* yielded the highest values among four of the seven measured parameters, which included *Sa* (1.91 ± 0.2 µm), *Sdr* (4.17 ± 0.21), *Sdq* (3.35 ± 0.090), and *Str* (0.90 ± 0.04). Moreover, *Sz* (21.00 ± 2.21 µm) and *Sku* (4.22 ± 0.46) were highest for *SB (Al)*, whereas *Ssk* (0.44 ± 0.15) was highest for *SB (Ti) AE* (Figure 3).

Bone cement-titanium shear test

The bone cement-titanium shear test results revealed that there were significant differences between the interfacial shear strengths of the surfaces. Compared with the *Ma* surface (20.55 N), the remaining treated surfaces exhibited greater interfacial shear strengths, as follows: the *SB (Al) AE* surface shear strength (81.45 N) greater by factor of 3.96 ($p<0.001$), *SB (Al)* surface shear strength (75.33 N) greater by factor of 3.67 ($p<0.001$), *SB (Ti) AE* surface shear strength (58.17 N) greater by a factor of 2.83 ($p<0.001$), and the *AE* surface shear strength (52.72 N) greater by a factor of 2.57 ($p<0.001$) (Figure 4).

Correlation between interfacial shear strength and surface roughness

The correlation between the interfacial shear strength values and the surface roughness parameters (*Sa, Sz, Sdr, Sdq, Str, Sku*, and *Ssk*) is shown in Figure 5. Moreover, *Sdr* (r=0.996), *Sdq* (r=0.982), and *Str* (r=0.969) exhibited significant correlation coefficients of 0.95 or greater, and *Sku* and *Ssk* did not exhibit a positive correlation.

Bone cement-titanium interfacial shear strength with respect to bonding area

From the evaluation of the interfaces with different bonding areas, no significant difference was found between the interfacial shear strength of the machined interface with a diameter of 2 mm (20.55 N) and the *SB (Al) AE* interface with a diameter of 1 mm (21.86 N) (Figure 6A). Similarly, no significant difference was found between the interfacial shear strength of the *SB (Al) AE* interface with a diameter of 2 mm (81.45 N) and the *AE* interface with a diameter of 2.5 mm (81.22 N) (Figure 6B).

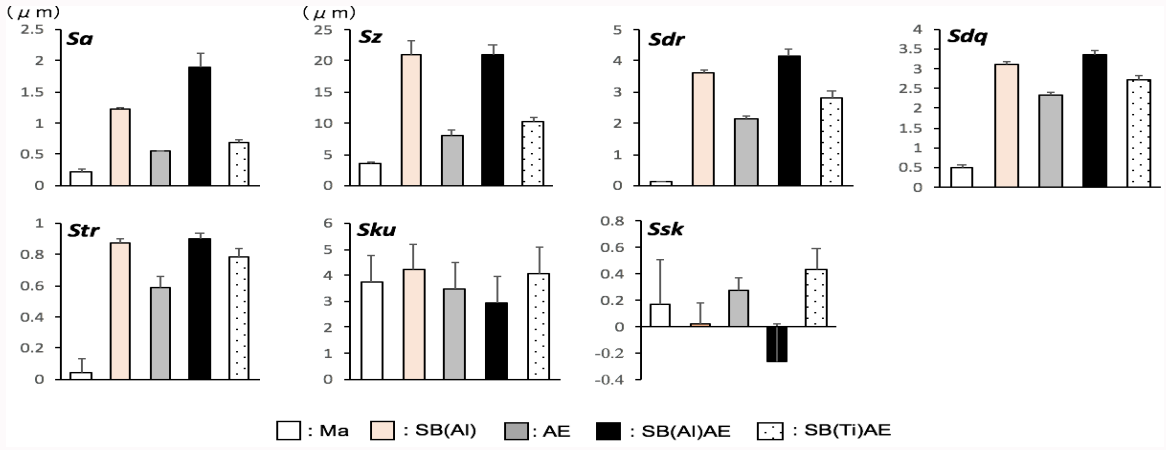

Figure 3: Quantitative measurement of surface roughness for *Ma, SB (Al), AE, SB (Al) AE*, and *SB (Ti) AE* titanium surfaces (*Sa, Sz, Sdr, Sdq, Str, Sku, and Ssk*). Each value represents the mean ± standard deviation of six sites on the five different surfaces (n=6). Texture aspect ratio.

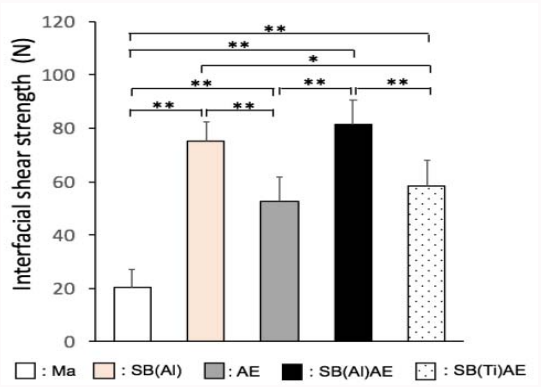

Figure 4: Measured bone cement-titanium interfacial shear strength of the *Ma, SB (Al), AE, SB (Al) AE*, and *SB (Ti) AE*. Data are presented as the mean ± SD (n=6). Statistically significance between each titanium surface and control: *p<0.01, **p<0.001.

Multiple regression analysis

The five topographical parameters that exhibited significant correlations with the interfacial shear strength are presented in Figure 7A. The correlation coefficients (r value) from highest to lowest were as follows: *Sdr, Sdq, Str, Sz*, and *Sa*. For the formulation of an equation that can best predict the interfacial shear strength, a multiple regression analysis was conducted using the five topographical parameters as explanatory variables. The effective explanatory variables were selected in accordance with the multiple regression analysis method, as follows:

a) Newly added variables are required to have a correlation coefficient higher than 0.996 (the correlation coefficient by a single regression of *(Sdr)*.

b) Variables are not significantly interdependent, thus preventing multicollinearity.

c) The positive or negative sign of a coefficient for each explanatory variable is required to match the positive or negative sign of the correlation coefficient (r) from its single regression analysis, respectively.

The resulting equation used to best predict the interfacial shear strength was as follows (Figure 7B): interfacial shear strength =9.14 *Sdr* + 5.99 *Sdq* + 4.65 *Sa* + 15.38 (r=0.997)

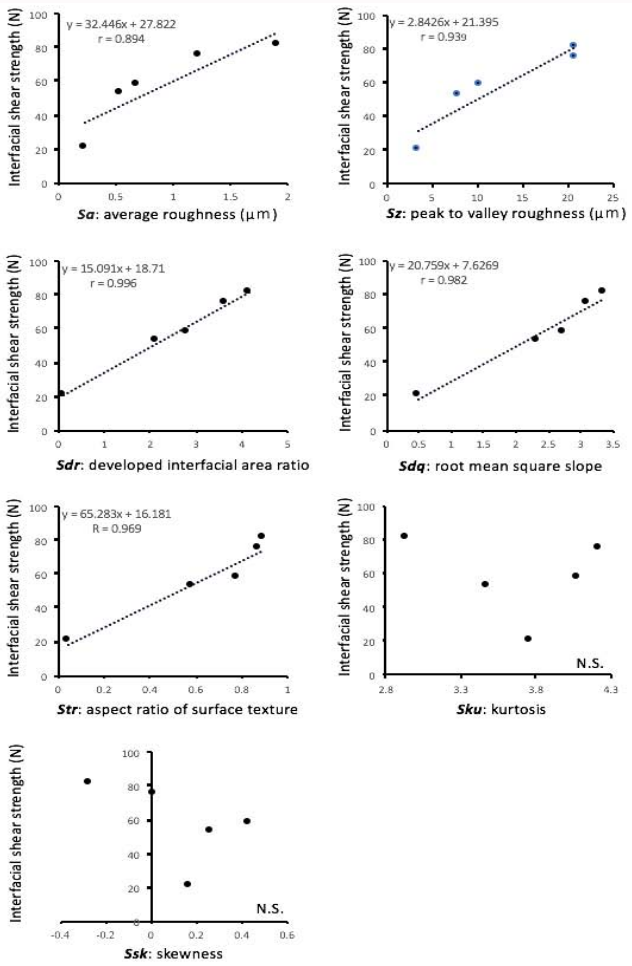

Figure 5: Linear equations and correlation coefficient between the shear stress test and the surface roughness (*Sa, Sz, Sdr, Sdq, Str, Sku*, and *Ssk*): statistically non-significant correlation.

The relative contributions of the variables that determine interfacial shear strength, as obtained from the analysis results, are presented in Figure 7; with *Sdr* as the major contributor (60%).

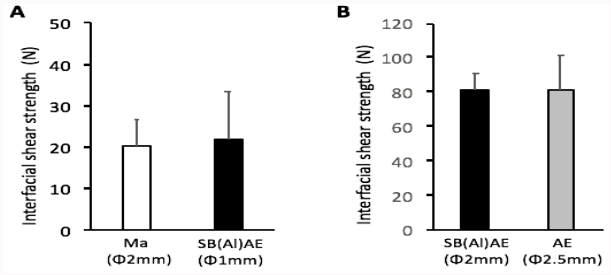

Figure 6: The evaluation of the interfaces with different bonding areas. At shear strength N, *Ma* (2 mm diameter) and *SB(Al)AE* (1 mm diameter) (a), at shear strength N, *SB(Al)AE* (2 mm diameter) and *AE* (2.5 mm diameter) (b), Data are shown as the mean ± SD (n=6). No statistically significant difference.

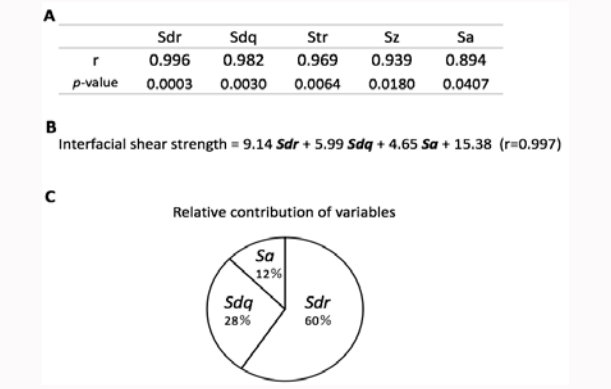

Figure 7: (A) Correlation coefficient between interface shear strength and surface roughness (*Sdr*, *Sdq*, *Str*, *Sz*, and *Sa*), (B) multiple regression equation of multiple correlation analysis, and (C) distribution of contribution degree.

Morphology of dissociated cement-titanium interface

Following the shear stress test, the morphologies of the bone cement-titanium interfaces were evaluated using SEM. At a low magnification (2500x), the images of the machined surfaces exhibited morphologies identical to their initial morphologies with concentric ridges. At a high magnification (20000x), several regions with thin layers of residual cement along the parallel ridge patterns were observed. The EDS spectra of the machined surface exhibited Ti (95%) and C (5%). Although unclear in the low magnification images (Figures 8A-8E); the high magnification images revealed that the titanium surfaces, which retained the cement material (Figures 8F-8J), were mostly entangled along the roughened peaks and filled the micron-level structures. On the *SB (Al) AE* surface, a cement layer that covered the majority of the titanium surface was observed (Figures 8K-8O). Moreover, the EDS spectra of *SB (Al) AE* exhibited Ti (44%) and C (56%).

Discussion

The use of dental implants is a standard and routine practice in various prosthodontic treatments. However, implant therapy is subject to significant scientific issues and unsolved clinical difficulties and limitations. Primary stability is critical for the successful execution of implant treatment. For an implant to demonstrate primary stability, it should resist movement, due to mechanical interlocking with the surrounding bone. Moreover, the realization of primary stability is significantly dependent on the skill level of the operator, amongst other factors. However, mechanical interlocking

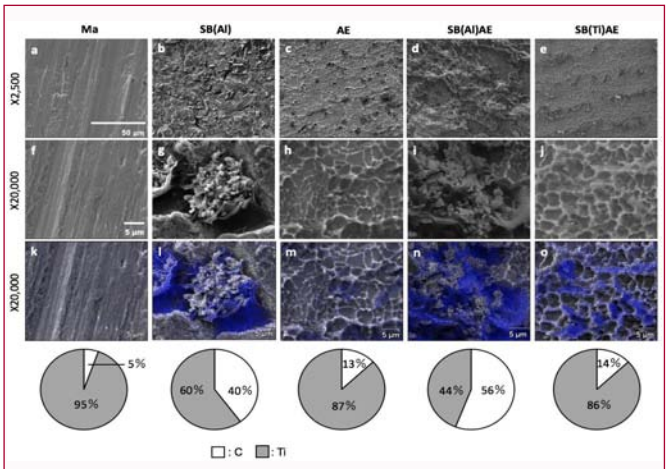

Figure 8: Morphology of detached cement-titanium interfaces and EDS results. Scanning electron micrographs of the (a,f) *Ma*, (b,g) *SB(Al)*, (c,h) *AE*, (d,i) *SB(Al)AE*, and (e,j) *SB(Ti)AE* surfaces. EDS results of the (k) *Ma*, (l) *SB(Al)*, (m) *AE*, (n) *SB(Al)AE*, and (o) *SB(Ti)AE*. Bar=50 μm in (a,b,c,d, and e), 5 μm in (f,g,h,i,j,k,l,m,n, and o). The pie chart presents the distribution of elements. C=carbon; Ti=titanium.

with bone at the microscopic scale is dependent on the morphology of the titanium implant surface. In addition to primary stability, the percentage of Bone-to-Implant Contact (BIC) was widely used to evaluate the extent to which titanium can be integrated with bone. However, bone tissue does not form entirely around implant surfaces, even in normal biological environments; which requires further research. According to the literature, the total implant area that is eventually covered by bone (bone-implant contact) remains at 45 ± 16% [16] or 50% to 75%, [17-19] which is significantly less than the ideal of 100%. Furthermore, it was determined whether the same BIC results in the same anchoring capacity of titanium implants. Thus, in this study, the effects of different titanium surface treatments and the interfacial shear strength using bone cement were evaluated.

Albrektsson and Wennerberg [20] classified four types of implant surface roughness: Smooth surface roughness (*Sa* <0.5 μm), minimally rough surface (*Sa* =0.5-1 μm), moderately rough surface (*Sa* =1 to 2 μm), and rough surface (*Sa* >2 μm). The surface-treated titanium samples used in this study can be classified as three types: smooth surface (machined), minimally rough surface *(AE* and *SB (Ti) AE)*, and moderately rough surface *(SB (Al)* and *SB (Al) AE)*. No significant differences were observed between the interfacial shear strengths of *AE* and *SB (Ti) AE*, and those between *SB (Al)* and *SB (Al) AE*. However, there were significant differences ($p<0.01$) between the surface types (smooth, minimally rough, and moderately rough). These findings suggest that there is a significant increase in the interfacial shear strength in accordance with an increase in the *Sa* value.

A comparison of the interfacial shear strengths of the five different surfaces indicated that the shear strength of the *Ma* surface was the lowest, and that of the *SB (Al) AE* surface was the highest. The interfacial shear strength can be improved by the use of roughened implant surfaces during the application of bone cement [21-23]. For example, blasted rough surfaces and chemically-treated porous surfaces generate high interfacial shear strengths [24-26]. In this study, the *SB (Al)* surfaces exhibited interfacial shear strengths that were greater than those of the *Ma* surfaces by factors of 4. Moreover, as observed, the resulting titanium surface roughness is dependent on the use of alumina or titanium particles. The *Sa* value of *SB (Al)*

AE (1.91 ± 0.2) was greater than that of *SB (Ti) AE* (0.69 ± 0.04) by a factor of 3 (Figure 3), and the *Sz* value of *SB (Al) AE* (21.00 ± 2.21) was greater than that of *SB (Ti) AE* (10.37 ± 0.57) by a factor of 2 (Figure 3). It was concluded that the surface roughness of titanium increased due to the use alumina particles, given their hardness.

With respect to the roughened surfaces, *SB (Al) AE* exhibited the highest value among four measurement parameters (*Sa, Sdr, Sdq*, and *Str*). Ordered from the most to least rough, the surfaces are as follows: *SB (Al) AE, SB (Al), SB (Ti) AE, AE*, and *Ma*. This order is identical to that of the interfacial shear strengths. In particular, there was a difference in the *Sa* values of *Ma* and *SB (Al) AE* surfaces in the order of 8.33. Moreover, there was a difference in the *Sz* values of the *Ma* and *SB (Al) AE* surfaces in the order of 6.07.

However, the single correlation analysis between the interfacial shear strength and surface roughness revealed that *Sdr* exhibited a high correlation (r=0.996). In addition, *Sdq, Str, Sz*, and *Sa* exhibited high correlation coefficients of 0.89 and greater. Hence, there was a high positive correlation between the interfacial shear strength and surface roughness.

Given that *SB (Al) AE* exhibited an interfacial shear strength that was greater than that of *Ma*, the influence of the surface area on the resulting shear strength was verified. With the bone cement columns with diameters of 2 mm, a surface area of 3.14 mm^2 was observed. A quarter of this area equals 0.785 mm^2, which corresponds to a column with a diameter of 1 mm. When comparing the interfacial shear strengths of *SB (Al) AE* (Φ1 mm) and *Ma* (Φ2 mm), no significant difference was observed, as expected. Moreover, *SB (Al) AE* had an interfacial shear strength that was greater than that of *AE* by a factor of approximately 1.5. The column area multiplied by 1.5 (3.14 mm^2) equates to 4.71 mm^2, which corresponds to a diameter of 2.5 mm. The resulting interfacial shear strengths of *SB (Al) AE* (Φ1 mm) and *AE* (Φ2.5 mm) were then compared, and no significant difference was observed. Thus, surfaces with different roughness characteristics require different BIC values to generate the same interfacial shear strength, thus verifying that the shear strength is not the same for the same BIC values.

To better understand the primary contributing factor to the shear strength, multiple regression analyses were conducted [26]. In particular, the response variable was considered as the interfacial shear strength, and the explanatory variable as the surface roughness. For explanatory variables, five positive correlation coefficients were used, as follows: *Sdr* (0.996), *Sdq* (0.982), *Str* (0.969), *Sz* (0.939), and *Sa* (0.894). The combination of the five or four explanatory variables and response variable was not analyzed. However, combinations of three explanatory variables, which begin with *Sdr, Sdq, Str*, and the response variable providing the following formula: Interfacial shear strength =14.55 *Sdr* + 12.86 *Sdq* - 38.82 *Str* + 13.77. The *Str* exhibited a negative partial regression coefficient and positive correlation coefficient.

With the combination of explanatory variables *Sdr, Sdq*, and *Sz,* and the response variable; the following formula was developed: Interfacial shear strength =3.63 *Sdr* + 10.47 *Sdq* + 0.88 *Sz* + 11.85. The standard partial regression coefficients were *Sdr* (24%), *Sdq* (48%), and *Sz* (28%). The correlation coefficient of *Sdr* was the maximum; however, the standard partial regression coefficient of the *Sdr* was the minimum.

With the combination of explanatory variables *Sdr, Sdq*, and *Sa*, and the response variable; the following formula was developed: interfacial shear strength =9.14 *Sdr* + 5.99 *Sdq* + 4.65 Sa +15.38. However, this combination did not exhibit multicollinearity. In this study, *Sdr* exhibited maximum values in the correlation coefficient and standard partial regression coefficient. Moreover, exhibited a high coefficient of 0.997. This equation indicates the relationship between the shear test values and three surface roughness parameters (*Sdr, Sdq, and Sa*). From the multiple regression analysis, *Sdr* was determined as the parameter that contributed most to the interfacial shear strength, with a contribution coefficient of 60%; whereas *Sa*, which is the most commonly used parameter in the field, contributed to only 12% of the interfacial shear strength. The *Sdr* is therefore a reliable parameter for the determination of the interlocking capacity of titanium with bone.

This paper presents a report on the application of *Ma, SB (Al), AE, SB (Al) AE,* and *SB (Ti) AE* on titanium surfaces and the influence of the surface morphology on the interfacial shear strength. The results were verified using SEM, in addition to an elemental composition analysis of the surfaces using EDS. The SEM images further confirmed that the shear occurred at the titanium-bone cement interface, and revealed that the mechanical interlocking due to a greater surface roughness was sufficiently strong to generate cohesive fractures within the bone cement columns. The SEM results revealed that the *SB (Al) AE* surfaces were associated with the highest percentage of residual bone cement after the shear test, thus indicating the infiltration of bone cement into the microstructures of the titanium surfaces. The *Ma* surface exhibited a significant lack of bone cement after the shear test, as further confirmed by EDS, with a high proportion of exposed titanium and as light amount of residual carbon. Moreover, *SB (Al) AE* exhibited bone-cement adhesion to the titanium surface, as represented by the proportion of carbon coverage indicated by the EDS imaging results.

Conclusion

In this study, significant differences in the mechanical interlocking capacity of titanium were observed with respect to different surface morphologies, thus indicating that the same BIC value does not directly correspond to the same anchoring capacity of titanium implants. Furthermore, the *Sdr* was found to be a highly reliable parameter that can be employed for the assessment of the interlocking capacity of titanium implant surfaces with respect to bone.

References

1. Albrektsson T, Branemark PI, Hansson HA, Lindstrom J. Osseointegrated titanium implants. Requirements for ensuring a long-lasting, direct bone-to-implant anchorage in man. Act Orthop Scand. 1981;52(2):155-70.
2. Ruffoni D, Wirth AJ, Steiner JA, Parkinson IH, Muller R, van Lenthe GH. The different contributions of cortical and trabecular bone to implant anchorage in a human vertebra. Bone. 2012;50(3):733-8.
3. Javed F, Romanos GE. The role of primary stability for successful immediate loading of dental implants. A literature review. J Dent. 2010;38(8):612-20.
4. Jemat A, Ghazali MJ, Razali M, Otsuka Y. Surface modifications and their effects on titanium dental implants. BioMed Res Int. 2015;2015:791725.
5. Jimbo R, Albrektsson T. Long-term clinical success of minimally and moderately rough oral implants: A review of 71 studies with 5 years or more of follow-up. Implant Dent. 2015;24(1):62-9.
6. Sammons RL, Lumbikanonda N, Gross M, Cantzler P. Comparison of osteoblast spreading on microstructured dental implant surfaces and cell behavior in an explant model of osseointegration: A scanning electron

microscopic study. Clin Oral Implants Res. 2005;16(6):657-66.

7. Buser D, Schenk RK, Steinemann S, Fiorellini JP, Fox CH, Stich H. Influence of surface characteristics on bone integration of titanium implants. A histomorphometric study in miniature pigs. J Biomed Mater Res. 1991;25(7):889-902.
8. Trisi P, Lazzara R, Rao W, Rebaudi A. Bone-implant contact and bone quality: Evaluation of expected and actual bone contact on machined and osseotite implant surfaces. Int J Periodontics Restorative Dent. 2002;22(6):535-45.
9. Molly L. Bone density and primary stability in implant therapy. Clin Oral Impt Res. 2006;17(Suppl 2):124-35.
10. Ito Y, Sato D, Yoneda S, Ito D, Kondo H, Kasugai S. Relevance of resonance frequency analysis to evaluate dental implant stability: Simulation and histomorphometrical animal experiments. Clin Oral Implants Res. 2008;19(1):9-14.
11. Degidi M, Perrotti V, Piattelli A, Lezzi G. Mineralized bone-implant contact and implant stability quotient in 16 human implants retrieved after early healing periods: A histological and histomorphometric evaluation. Int J Oral Maxillofac Implants. 2010;25(1):45-8.
12. Al-Nawas B, Groetz KA, Goetz H, Duschner H, Wagner W. Comparative histomorphometry and resonance frequency analysis of implants with moderately rough surfaces in a loaded animal model. Clin Oral Implants Res. 2008;19:1-8.
13. Wong M, Eulenberger J, Schenk R, Hunziker E. Effect of surface topology on the osseointegration of implant materials in trabecular bone. J Biomed Mater Res. 1995;29(12):1567-75.
14. Wennerberg A, Albrektsson T. On implant surfaces: A review of current knowledge and opinions. Int J Oral Maxillofac Implants. 2010;25(1):63-74.
15. Webb JC, Spencer RF. The role of polymethylmethacrylate bone cement in modern orthopaedic surgery. J Bone Joint Surg Br. 2007;89(7):851-7.
16. Weinlaender M, Kenney EB, Lekovic V, Beumer J, Moy PK, Lewis S. Histomorphometry of bone apposition around three types of endosseous dental implants. Int J Oral Maxillofac Implants. 1992;7(4):491-6.
17. Berglundh T, Abrahamsson I, Albouy JP, Lindhe J. Bone healing at implants with a fluoride-modified surface: an experimental study in dogs. Clin Oral Impl Res. 2007;18(2):147-52.
18. Ogawa T, Nishimura I. Different bone integration profiles of turned and acid-etched implants associated with modulated expression of extracellular matrix genes. Int J Oral Maxillofac Implants. 2003;18(2):200-10.
19. De Maeztu MA, Braceras I, Alava JI, Gay-Escoda C. Improvement of osseointegration of titanium dental implant surfaces modified with CO ions: a comparative hisomorphometric study in beagle dogs. Int J Oral Maxillofac Implants. 2008;37(5):441-7.
20. Albrektsson T, Wennerberg A. Oral implant surfaces: Part 2-review focusing on clinical knowledge of different surfaces. Int J Prosthodont. 2004;17(5):544-64.
21. Mulroy WF, Estok DM, Harris WH. Total hip arthroplasty with use of so-called second-generation cementing techniques. A fifteen-year-average follow-up study. J Bone Joint Surg Am. 1995;77(12):1845-52.
22. Sanchez-Sotelo J, Berry DJ, Harmsen S. Long-term results of use of a collared matte-finished femoral component fixed with second-generation cementing techniques. J Bone Joint Surg Am. 2002;84(9):1636-41.
23. Mulroy WF, Harris WH. Revision total hip arthroplasty with use of so-called second-generation cementing techniques for aseptic loosening of the femoral component. A fifteen-year-average follow-up study. J Bone Joint Surg Am. 1996;78(3):325-30.
24. Muller RT, Schurmann N. Shear strength of the cement metal interface - an experimental study. Arch Orthop Trauma Surg. 1999;119(3-4):133-8.
25. Davies JP, Harris WH. *In vitro* and *in vivo* studies of pressurization of femoral cement in total hip arthroplasty. J Arthroplasty. 1993;8(6):585-91.
26. Chen PC, Pinto JG, Mead EH, D'Lima DD, Colwell CW. Fatigue model to characterize cement–metal interface in dynamic shear. Clin Orthop Relat Res. 1998;350:229-36.